Journal of Nepal Mathematical Society (JNMS)
ISSN: 2616-0153 (Print), 2616-0161 (Online)
Vol. 7, Issue 1, 2024 (July): 14-31
DOI: https://doi.org/10.3126/jnms.v7i1.67586

Research Article
Received Date: May 14, 2024
Accepted Date: June 12, 2024
Published Date: July 03, 2024

Transmission Dynamics of Dengue Disease in the Rupandehi District of Nepal

Dwarika Prasad Gautam[1], Ramesh Gautam[2,6,*], Khagendra Adhikari[3,6], Anjana Pokharel[4,6], Kedar Nath Uprety[5,6]

[1]Lumbini Banijya Campus, Butwal, Nepal
[2]Ratna Rajya Laxmi Campus, Tribhuvan University, Kathmandu, Nepal
[3]Amrit Science Campus, Tribhuvan University, Kathmandu, Nepal
[4]Padma Kanya Multiple Campus, Tribhuvan University, Kathmandu, Nepal
[5]Central Department of Mathematics, Tribhuvan University, Kathmandu, Nepal
[6]Mathematical Biology Research Center (MBRC), Nepal

*Correspondence to: Ramesh Gautam, Email: *rgnumberth79@gmail.com*

Abstract: *Increasing incidence of dengue fever has become an important health concern in recent years, especially in developing country like Nepal. To investigate patterns of transmission, this work uses a mathematical model for the dynamics of dengue outbreaks in the Rupandehi district in 2017. To validate the model biologically, we demonstrate the positivity and boundedness of solutions. Furthermore, we establish that for $R_0 < 1$, the disease-free equilibrium is locally asymptotically stable, whereas for $R_0 > 1$, a unique endemic equilibrium point exists. Sensitivity analysis showed that the parameters related to mosquitoes, in particular the mosquito death rate (μ_v) and mosquito biting rate in transmission rates ($\beta_1, \beta_2, \beta_v$), have significant impact on R_0. Therefore, implementing mosquito control activities followed by protection against mosquito bites are crucial strategies in effectively controlling dengue transmission.*

Keywords: Dengue, Reproduction number, Endemic equilibrium, Rupandehi district

1 Introduction

Dengue is a viral infection transmitted through the bites of infected female Aedes aegypti mosquitoes that carry the dengue virus [27]. The four strains of the dengue virus are DEN1, DEN2, DEN3, and DEN4 [6, 11, 14]. Even though individual may develop immunity to one serotype of the dengue virus after being infected, they can still be susceptible to infection by the other three serotypes [9]. In dengue disease, symptoms typically appear within one to seven days after being bitten by an infected mosquito. Common symptoms include fever, headache, muscle and joint pain, pain behind the eyes, abdominal discomfort, nausea, vomiting, mucosal bleeding, and rashes [27].

The first recognized dengue epidemics emerged almost simultaneously in Asia, Africa and North America during the 1780s. Since then, dengue has spread across tropical and subtropical regions worldwide, becoming prevalent in urban and semi-urban areas [17]. In the recent years, the incidence of dengue cases has significantly risen, placing over half of the world's population at risk [27]. The World Health Organization (WHO) estimates that annually, there are between 100 to 400 million dengue infections worldwide, with more than 8 out of 10 cases being generally mild and asymptomatic [27]. Over four million cases and more than four thousand dengue-related deaths were reported from 80 countries globally in 2023 [23].

In the context of Nepal, the first case of dengue was identified in 2004 [25]. According to the Epidemiology and Disease Control Division (EDCD) under the Ministry of Health and Population (MoHP), government of Nepal, dengue infections were reported across all seven provinces and 77 districts in 2022, totaling 54,784 cases. Among these, Lumbini Province alone reported 5,037 cases [24]. Particularly, in Rupandehi district as of 2022, the number of dengue cases had surged to 1215, positioning it as the eighth highest among the 77 districts nationwide [15]. According to the District Public Health Office (DPHO) of Rupandehi, the first dengue outbreak in the district was recorded in 2010, resulting in 21 reported cases, which is the main concern of this study [23]. Dengue outbreaks in Nepal often result from a combination of factors, including climate change, unplanned urban development, insufficient solid waste management, easy transit between

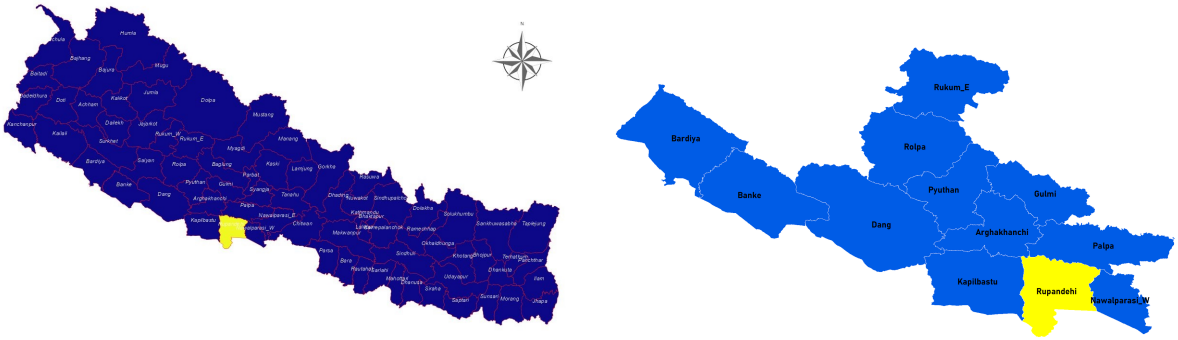

(a) (b)

Figure 1: The map of Nepal has been crafted using data sourced from the official website of the Government of Nepal (`http:/httpdos.gov.np`). Utilizing the R 4.3.1 software, specifically employing the cartography package, the map highlights the Rupandehi district. Within the map, Rupandehi district is distinctly represented by a vibrant yellow hue, ensuring clear visibility and recognition of its geographical boundaries.

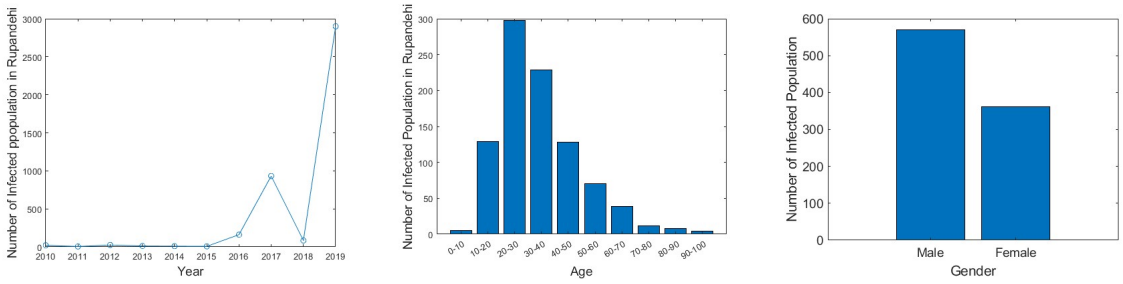

(a) (b) (c)

Figure 2: (a) Annual infected individuals (b) Breakdown of infected persons by age group (c) Distribution of infected individuals by gender in Rupandehi district during 2017 [21, 23, 24].

dengue-prone areas and limited public health resources [24].

Rupandehi district (Figure 1(b)) is situated within the Lumbini Province of Nepal and is renowned worldwide as the sacred birthplace of Lord Gautam Buddha, the pioneer of world peace. With an elevation ranging from 100 to 1229 meters above sea level, Rupandehi spans a total area of 1360 square kilometers. The district experiences a temperature range between 45.4^0 (maximum) and $8.75^0 c$ (minimum).

Figure 2(a) illustrates the yearly trend of dengue infection from 2010 to 2019, revealing a notable increase in disease incidence in recent years. This escalating trend underscores the urgent need for effective control measures to mitigate morbidity and mortality rates. Furthermore, Figure. 2(b) indicates that dengue fever predominantly affects individuals within the active age group of 15-60 years. This could be attributed to their propensity for outdoor activities, increasing their exposure to mosquito bites. Additionally, Figure 2(c) presents the distribution of dengue cases by gender in Rupandehi district in 2017, highlighting a higher proportion of infections among males.

Mathematical modeling in epidemiology is an important tool to understand the dynamics of diseases and control strategies [1, 2, 3, 5, 8, 15, 20]. Moreover, it provides valuable insights for policymakers and public health authorities to make informed decisions and effectively control disease outbreaks. In the history of mathematical modeling, the basic SIR model (S: Susceptible, I: Infected, and R: Recovered) is developed by Kermack and Kendrick in 1927 [13], which described the threshold condition for epidemics which

concluded that an epidemic would not occur if the population density remained below the threshold value. The first mathematical model describing dengue fever dynamics was found, dating back to 1970 [4]. Fischer and Halstead [7] examined the correlation between the pathogenesis of dengue hemorrhagic fever and investigated the rates of sequential infection based on antibody specificity, employing a mathematical model. However in 1998, Esteva and Vargas developed a disease transmission model incorporating interactions between human and vector populations [6] and provided insights into the dynamics of disease transmission in such contexts. Rodrigues et al. [19] presented a comprehensive model for dengue transmission, featuring eight mutually exclusive compartments representing human and vector dynamics. They identified three possible equilibria: two disease-free equilibria (DFE) and another endemic equilibrium. Their study included a case analysis of the 2009 dengue outbreak in Cape Verde. Vaidya and Wang [20] constructed a mathematical model to explore the influence of seasonal and diurnal temperature fluctuations on the persistence of the mosquito vector and dengue transmission. Their study yielded novel insights into the theoretical comprehension of the role played by diurnal temperature variations. These insights could potentially aid in the control of mosquito vectors and consequently, the spread of the dengue virus. Josh et al. [10] developed and thoroughly examined a deterministic mathematical model to describe the transmission dynamics of co-infection with the Zika virus and Dengue fever. Kafle et al. [12] used the SEIR compartmental model to investigate the transmission dynamics of dengue disease and analyzed the influence of temperature on dengue transmission dynamics.

The key contributions of this paper are as follows:

- The data of dengue disease in Rupandehi district indicates that there is a noticeable variation in the distribution of dengue diseases across different age groups.
- To the best of our understanding, there is currently no existing literature that investigates the dynamics of dengue disease through the use of a mathematical model in the context of the Rupandehi district. Therefore, we have developed a model to examine the dynamics of dengue disease specifically in the Rupandehi district of Nepal.
- We have developed an epidemiological model termed $S_H S_L EIR{-}SEI$. A comprehensive examination of the transmission dynamics of a dengue disease model is conducted.
- The basic reproduction number is calculated using the next generation matrix method.
- The effective parameters influencing disease spread are identified and analyzed using MATLAB and MATHEMATICA for numerical simulation.

2 Methods

2.1 Model formulation

We have developed a mathematical model that describes the risk-based dynamics of dengue disease while accounting for a range of age groups. There are five distinct compartments of the human population (N_h): low-risk susceptible (S_{Lh}), high-risk susceptible (S_{Hh}), exposed (E_h), infected (I_h), and recovered (R_h). In addition, the population of mosquitoes is divided into three groups: susceptible (S_v), exposed (E_v), and infectious (I_v). The primary method of dengue transmission is mosquito bites; vulnerable people catch the virus from infected humans through infectious mosquitoes. As a function of human risk, the rates of transmission from infected mosquitoes to susceptible humans are β_1 and β_2, respectively.

In addition, β_v represents the transmission rate from infectious humans to susceptible mosquitoes. Furthermore, the parameters Γ_h and Γ_v represent the recruitment rates of human and mosquito populations, respectively. The parameters μ_h and μ_v denote the natural death rates of the human and mosquito populations, while γ_h represents the recovery rate of the infectious human population. The parameter σ denotes the progression rate of exposed humans to infectious individuals with clinical symptoms, while ζ represents the progression rate of mosquitoes from the exposed to the infectious state. Moreover, the parameters η and θ represent the mobility rates of individuals from high-risk to low-risk susceptible and from low-risk to high-risk susceptible, respectively. The schematic diagram of the model is shown in Figure 3.

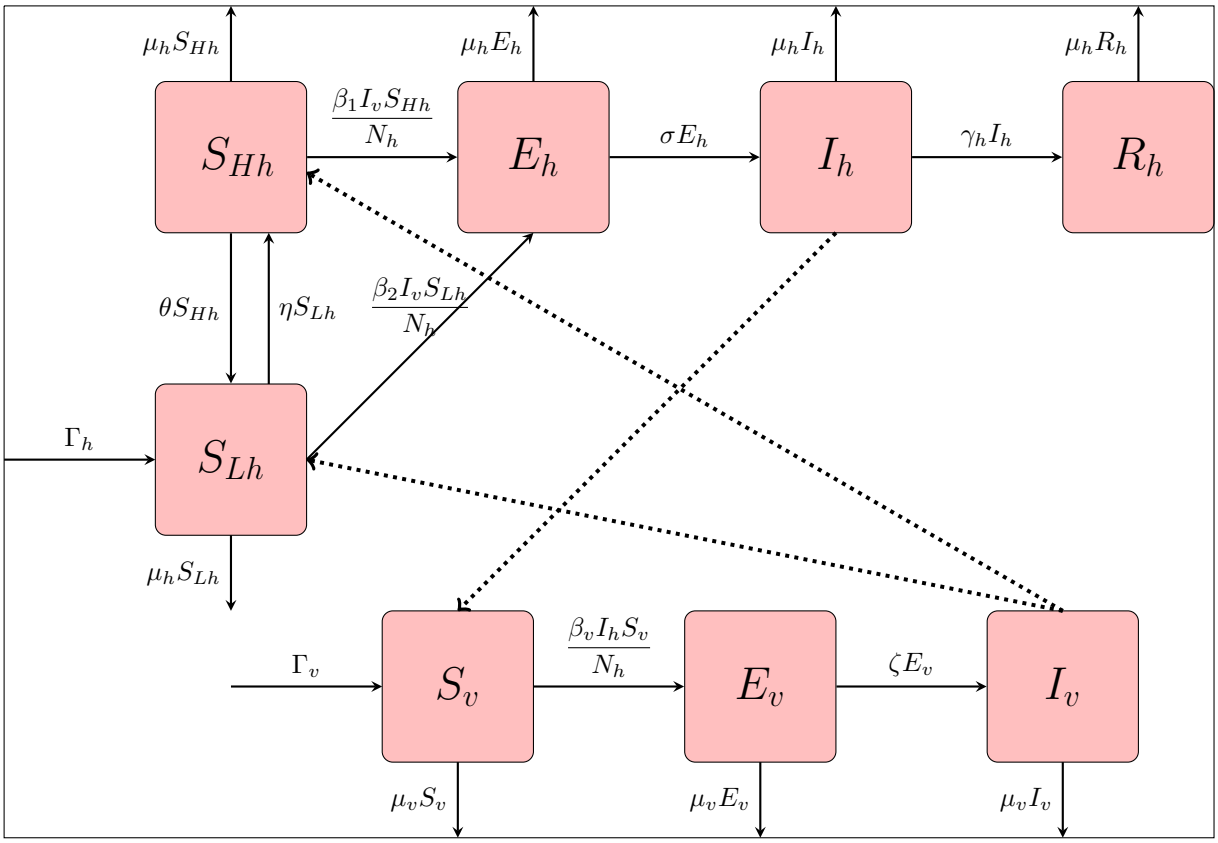

Figure 3: Schematic diagram of mathematical model of dengue disease considering low and high risk humans in Rupandehi districts. Here, subscripts h and v refer to human and mosquito respectively and the subscripts L and H refer to the low risk and high risk humans population respectively.

The transmission model of dengue disease can be described by the following system of differential equations:

$$\frac{dS_{Hh}}{dt} = \eta S_{Lh} - \frac{\beta_1 S_{Hh} I_v}{N_h} - (\mu_h + \theta) S_{Hh}, \tag{1}$$

$$\frac{dS_{Lh}}{dt} = \Gamma_h - \frac{\beta_2 S_{Lh} I_v}{N_h} - (\eta + \mu_h) S_{Lh} + \theta S_{Hh}, \tag{2}$$

$$\frac{dE_h}{dt} = \frac{\beta_1 S_{Hh} I_v}{N_h} + \frac{\beta_2 S_{Lh} I_v}{N_h} - (\mu_h + \sigma) E_h, \tag{3}$$

$$\frac{dI_h}{dt} = \sigma E_h - (\mu_h + \gamma_h) I_h, \tag{4}$$

$$\frac{dR_h}{dt} = \gamma_h I_h - \mu_h R_h, \tag{5}$$

$$\frac{dS_v}{dt} = \Gamma_v - \frac{\beta_v S_v I_h}{N_h} - \mu_v S_v, \tag{6}$$

$$\frac{dE_v}{dt} = \frac{\beta_v S_v I_h}{N_h} - (\mu_v + \zeta) E_v, \tag{7}$$

$$\frac{dI_v}{dt} = \zeta E_v - \mu_v I_v. \tag{8}$$

2.2 Data source

This study utilized dengue disease data from Rupandehi district, focusing on daily data from the year 2017 to fit the model. The dengue case data were sourced from the District Public Health Office (DPHO) of Rupandehi.

2.3 Estimation of parameters

The population of Rupandehi district in 2017 was predicted to be 1,015,634 [24]. Therefore, the initial value of $N_h(0)$ was estimated to be 1,015,634. The population was divided into high and low-level categories, with percentages of 53.9% and 46.1%, respectively [24]. Given that dengue cases were limited to a small number of palikas, it is logical to infer that only a portion, represented by α, of the entire population was part of the dengue transmission contact network. Thus, the population in the contact network is denoted as $\alpha N_h(0)$. Using this information, the starting quantities of persons in separate compartments may be computed as follows: $S_{Lh}(0) = 0.461 \times \alpha 1015614 = \alpha 468206, S_{Hh}(0) = 0.539 \times \alpha 1015614 = \alpha 468198, R_h(0) = 0, I_h(0) = 10, E_h(0) = 10$.

The Crude Birth Rate (CBR) in Rupandehi District is reported as 22, indicating the annual number of live births per 1000 individuals [24]. The human recruitment rate per day for the population in the low-level susceptible group, denoted by Γ_h, can be estimated using the formula $\Gamma_h = \alpha \dfrac{22 \times 1015634}{1000 \times 365}$, which simplifies to α 61 per day. The average life expectancy of Rupandehi is 68.8 years, which translates to a natural mortality rate of people, represented by μ_h, is estimated as $\dfrac{1}{68.8 \times 365} = 0.000039857$ per day [24]. In addition, the recovery period of infectious individual is 7 days [6], so the recovery rate, represented by γ_h, is determined to be $\dfrac{1}{7} = 0.1428$ per day and the rate of humans from exposed to infectious class(σ)=0.1429 per day[27].

We assumed the mosquito population is equivalent to the human population because female mosquito populations have been estimated to be 1–10 times larger than human populations [8]. The entire population of mosquitoes is thus split up into different compartments, giving $S_v(0) = \alpha 1015134$, $E_v(0) = 20$, and $I_v(0) = 30$. Since individuals in the low susceptible group stay for 15 years, whereas those in the high susceptible group stay for 45 years, we can assume the following parameters: $\theta = 0.000060883$ per day, $\eta = 0.00018265$ per day, and $\zeta = 0.2$ per day [24]. Data fitting is used to estimate the remaining parameters, which are β_1, β_2, β_v and α.

2.4 Data fitting

We utilized the methodology outlined in the previous study by Rahaman et al. [17] to conduct the data fitting process. The data set used for model fitting comprises the daily count of newly reported cases of infected individuals. The equation

$$L(t) = \phi \sigma E_h,$$

where ϕ, representing the proportion of infections that are recorded, is estimated through the data fitting process, allowing for the computation of the recorded new infections generated at time t, denoted as $L(t)$.

We solved the system of differential equations numerically using a fourth order Runge–Kutta method. We used the solutions to obtain the best-fit parameters via a nonlinear least squares regression method that minimizes the following sum of the squared residuals

$$J(\beta_1, \beta_2, \beta_v, \alpha, \phi) = \sum_{i=1}^{n} (L(t_i) - \bar{L}(t_i))^2,$$

where $\beta_1, \beta_2, \beta_v, \alpha, \phi$ are parameters to be estimated, and $L(t_i)$, and $\bar{L}(t_i)$ are the new cases of recorded infectious people predicted by the model and those given in the available data, respectively. Here, n represents the total number of data points used for the model fitting.

2.5 Epidemic pattern and model validation

From September 27 to December 7, 2017, we used daily recorded new case data from the Rupandehi district to fit our model. The estimated five parameters, $\beta_1, \beta_2, \beta_v, \alpha$ and ϕ are shown in Table 2. The model has an excellent level of precision with the data from new reported cases, as shown in Figure 4. Furthermore, we estimated the cumulative dengue cases during the study period using our model and cross-checked our results with the data shown in Figure 4. Our modeling approach is validated by the fact that our model may predict the cumulative cases of dengue in Rupandehi with accuracy.

Table 1: Base value of demographic variables of dengue in Rupandehi

Description	**State Variables**	**Base Value**	**Reference**
Population of Rupandehi District in 2017	$N_h(0)$	1015634	[24]
Low risk Susceptible Population in Rupandehi	$S_{Lh}(0)$	468198	Calculated
High risk Susceptible Population in Rupandehi	$S_{Hh}(0)$	547516	Calculated
Recovered Population in Rupandehi	$R_h(0)$	0	Assumed
Infected Population in Rupandehi	$I_h(0)$	10	[22]
Exposed Population in Rupandehi	$E_h(0)$	10	Assumed
Population of mosquitoes in Rupandehi	$S_v(0)$	1015634	Assumed
Infected mosquitoes	$I_v(0)$	30	Assumed
Exposed Population of mosquitoes in Rupandehi	$E_v(0)$	20	Assumed

Table 2: Values and range of the parameters of the model

Description	**Parameters**	**Base Values/unit**	**Reference**
Death rate of human	μ_h	0.000039857 per day	[26]
Death rate of mosquito	μ_v	0.1250 per day	[6]
Transmission rate from mosquito to mosquito	β_v	0.376 per day	Estimated
Transmission rate from mosquito to high risk susceptible humans	β_1	0.66 per day	Estimated
Transmission rate from mosquito to low risk susceptible humans	β_2	0.5 per day	Estimated
Rate of mosquito from exposed to infectious class	ζ	0.2 per day	Assumed
Mobility rate of humans from low risk to high risk susceptible	θ	0.000060883 per day	Calculated
Recruitment rate of humans	Γ_h	0.3528 per day	Calculated
Recruitment rate of mosquitoes	Γ_v	1110 per day	Assumed
Mobility rate of humans from high risk to low risk susceptible	η	0.00018265 per day	Calculated
Recovery rate of human populations	γ_h	0.1428 per day	[6]
Rate of humans from exposed to infectious class	σ	0.1429 per day	[24]
Portion of the total population	α	1/115	Estimated
proportion of recorded infections	ϕ	0.10335	Estimated

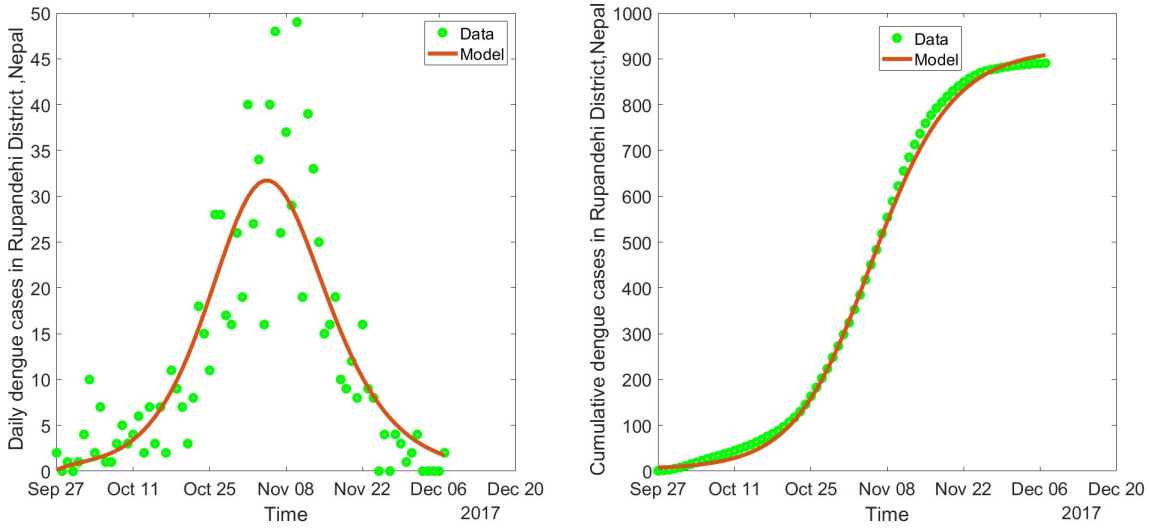

(a) (b)

Figure 4: *Data fitting and model validation:* (a) Plot displaying the recorded daily new cases of dengue data (circles) overlaid with the best-fit model prediction (line) (b) Representation of cumulative cases over the entire study period estimated by the model (line), juxtaposed with the actual data points (circles) from Rupandehi district in 2017.

3 Model Analysis

3.1 Positivity and boundedness of solutions

In this section, it is shown that the solution of all the state variables are always positive and bounded when the initial conditions are positive. This serves to illustrate the model is well-posed.

Theorem 1. *For all positive initial data, the solution set of the system is always positive and bounded.*

Proof. Here, we use the contradiction approach to establish the theorem. Suppose $S_{Hh}(t) > 0$ is not possible for all $t > 0$ and there exists $t = t_1 > 0$ is the first time point such that $S_{Hh}(t_1) = 0$. Now from the Eq.(1) of the system $\frac{dS_{Hh}}{dt}|_{t=t_1} = \eta S_{Lh}(t_1)$. Now, we claim that $S_{Lh}(t_1)$ can not be negative.
Suppose, if possible there exists first time point $0 < t_2 < t_1$ such that $S_{Lh}(t_2) = 0$. It follows from the Eq.(2), $\frac{dS_{Lh}}{dt}|_{t=t_2} = \Gamma_h + \theta S_{Hh}(t_2) > 0 \quad (t_2 < t_1 \text{ and } S_{Hh}(t_1) = 0)$. It follows that there exists $\epsilon > 0$ such that $S_{Lh}(t) < 0$ for $0 < t < t_2 - \epsilon$ and contradicts our assumption that t_2 is the first time for which $S_{Lh}(t_2) = 0$. Therefore $S_{Lh}(t_2) > 0$ and hence $S_{Lh}(t_1)$ cannot be negative. Therefore, $S'_{Hh}(t_1) > 0$ and again contradicts $S_{Hh}(t_1) = 0$. Therefore $S_{Hh}(t) > 0$ for all t. Similarly, we can show that $S_{Lh}, E_h, I_h, R_h, S_v$ and I_v are positive.

Now we show all the solutions are bounded forever. Here, $N_h = S_{Hh} + S_{Lh} + E_h + I_h + R_h$.
Now adding equations of human compartments, we have

$$\begin{aligned}
\frac{dN_h}{dt} &= \frac{dS_{Hh}}{dt} + \frac{dS_{Lh}}{dt} + \frac{dE_h}{dt} + \frac{dI_h}{dt} + \frac{dR_h}{dt} \\
or, \frac{dN_h}{dt} &= \Gamma_h - \mu_h(S_{Hh} + S_{Lh} + E_h + I_h + R_h) \\
or, \frac{dN_h}{dt} &= \Gamma_h - \mu_h N_h \\
or, \frac{dN_h}{dt} + \mu_h N_h &= \Gamma_h \\
or, [N_h e^{\mu_h t}]_0^t &= \int_0^t \Gamma_h e^{\mu_h t} dt \\
or, [N_h e^{\mu_h t}]_0^t &= \frac{\Gamma_h}{\mu_h} e^{\mu_h t} - \frac{\Gamma_h}{\mu_h} \\
or, N_h(t) &= N_h(0) e^{-\mu_h t} + \frac{\Gamma_h}{\mu_h} - \frac{\Gamma_h}{\mu_h} e^{-\mu_h t}.
\end{aligned}$$

which implies $N_h(t) = \frac{\Gamma_h}{\mu_h}$ as $t \to \infty$. $\therefore N_h(t)$ is bounded.

Similarly ,we can show that $S_{Hh}(t), S_{Lh}(t), E_h, I_h, R_h, S_v, E_v, I_v$ are bounded. □

3.2 Disease free equilibrium

Now, the disease-free equilibrium is obtained by setting $\frac{dS_{Hh}}{dt} = 0$, $\frac{dS_{Lh}}{dt} = 0$, $\frac{dE_h}{dt} = 0$, $\frac{dI_h}{dt} = 0$, $\frac{dR_h}{dt} = 0$, $\frac{dS_v}{dt} = 0$, $\frac{dE_v}{dt} = 0$, $\frac{dI_v}{dt} = 0$ together with $I_h = 0$ and $I_v = 0$.

It follows that the disease-free equilibrium of the system

$$E^0 = \left(\frac{\eta\Gamma_h}{\mu_h(\eta + \theta + \mu_h)}, \frac{\Gamma_h(\theta + \mu_h)}{\mu_h(\eta + \theta + \mu_h)}, 0, 0, 0, \frac{\Gamma_v}{\mu_v}, 0, 0 \right)$$

3.3 Basic reproduction number

Basic reproduction number is defined as the average number of secondary infectious caused by a single infectious individual during their entire infectious life time in a completely susceptible population. It is denoted by R_0. It forecasts whether a disease will die out or becomes endemic. Using the next generation method, we computed the associated reproduction number of the model which is defined as $R_0 = \rho(FV^{-1})$.

Where, F= transmission matrix, V = transition matrix.

The infectious subsystem is deduced from above equations as

$$\frac{dE_h}{dt} = \frac{\beta_1 S_{Hh} I_v}{N_h} + \frac{\beta_2 S_{Lh} I_v}{N_h} - (\mu_h + \sigma)E_h, \tag{9}$$

$$\frac{dI_h}{dt} = \sigma E_h - (\mu_h + \gamma_h)I_h, \tag{10}$$

$$\frac{dE_v}{dt} = \frac{\beta_v S_v I_h}{N_h} - (\mu_v + \zeta)E_v, \tag{11}$$

$$\frac{dI_v}{dt} = \zeta E_v - \mu_v I_v. \tag{12}$$

Then the Jacobian matrix from the Eqs (9–12) is computed as

$$J(E_h, I_h, E_v, I_v) = \begin{pmatrix} \mu_h + \sigma & 0 & 0 & \frac{\beta_1 S_{Hh}}{N_h} + \frac{\beta_2 S_{Lh}}{N_h} \\ \sigma & \mu_h + \gamma_h & 0 & 0 \\ 0 & \frac{\beta_v S_v}{N_h} & \mu_v + \zeta & 0 \\ 0 & 0 & \zeta & \mu_v \end{pmatrix}$$

The Jacobian matrix is decomposed into two matrices

$$V = \begin{pmatrix} \mu_h+\sigma & 0 & 0 & 0 \\ -\sigma & \mu_h+\gamma_h & 0 & 0 \\ 0 & 0 & \mu_v+\zeta & 0 \\ 0 & 0 & -\zeta & \mu_v \end{pmatrix} \text{ and } F = \begin{pmatrix} 0 & 0 & 0 & \frac{\beta_1 S_{Hh}}{N_h}+\frac{\beta_2 S_{Lh}}{N_h} \\ 0 & 0 & 0 & 0 \\ 0 & \frac{\beta_v S_v}{N_h} & 0 & 0 \\ 0 & 0 & 0 & 0 \end{pmatrix}.$$

$$\text{Now, } V^{-1} = \begin{pmatrix} \frac{1}{(\sigma+\mu_h)} & 0 & 0 & 0 \\ -\frac{\sigma}{(\sigma+\mu_h)(\gamma_h+\mu_h)} & \frac{1}{\gamma_h+\mu_h} & 0 & 0 \\ 0 & 0 & \frac{1}{\zeta+\mu_v} & 0 \\ 0 & 0 & -\frac{\zeta}{\mu_v(\zeta+\mu_v} & \frac{1}{\mu_v} \end{pmatrix}$$

At the disease-free equilibrium point $\left(\frac{\eta\Gamma_h}{\mu_h(\eta+\theta+\mu_h)}, \frac{\Gamma_h(\theta+\mu_h)}{\mu_h(\eta+\theta+\mu_h)}, 0, 0, 0, \frac{\Gamma_v}{\mu_v}, 0, 0\right)$,

$$\text{The newly infectious matrix: } F = \begin{pmatrix} 0 & 0 & 0 & \frac{(\eta\beta_1+\beta_2(\theta+\mu_h))}{(\eta+\theta+\mu_h)} \\ 0 & 0 & 0 & 0 \\ 0 & \frac{\Gamma_v\beta_v\mu_v}{\Gamma_h\mu_v} & 0 & 0 \\ 0 & 0 & 0 & 0 \end{pmatrix}.$$

$$\therefore FV^{-1} = \begin{pmatrix} 0 & 0 & -\frac{\zeta(\eta\beta_1+\beta_2(\theta+\mu_h))}{\mu_v(\eta+\theta+\mu_h)(\zeta+\mu_v)} & \frac{(\eta\beta_1+\beta_2)(\theta+\mu_h)}{\mu_v(\eta+\theta+\mu_h)} \\ 0 & 0 & 0 & 0 \\ -\frac{\Gamma_v\sigma\beta_v\mu_h}{\Gamma_h(\sigma+\mu_h)(\gamma_h+\mu_h)\mu_v} & \frac{\Gamma_v\beta_v\mu_h}{\Gamma_h(\gamma_h+\mu_h)\mu_v} & 0 & 0 \\ 0 & 0 & 0 & 0 \end{pmatrix}.$$

The characteristic equation of above matrix is $\left|FV^{-1}-\lambda I\right| = 0$

$$\text{or, } \begin{vmatrix} -\lambda & 0 & -\frac{\zeta(\eta\beta_1+\beta_2(\theta+\mu_h))}{\mu_v(\eta+\theta+\mu_h)(\zeta+\mu_v)} & \frac{(\eta\beta_1+\beta_2)(\theta+\mu_h)}{\mu_v(\eta+\theta+\mu_h)} \\ 0 & -\lambda & 0 & 0 \\ -\frac{\Gamma_v\sigma\beta_v\mu_h}{\Gamma_h(\sigma+\mu_h)(\gamma_h+\mu_h)\mu_v} & \frac{\Gamma_v\beta_v\mu_h}{\Gamma_h(\gamma_h+\mu_h)\mu_v} & -\lambda & 0 \\ 0 & 0 & 0 & -\lambda \end{vmatrix} = 0.$$

$$\therefore \lambda = \pm\sqrt{\frac{\zeta\mu_h\sigma\beta_v\Gamma_v(\eta\beta_1+\beta_2(\theta+\mu_h))}{\Gamma_h\mu_v^2(\eta+\theta+\mu_h)(\sigma+\mu_h)(\gamma_h+\mu_h)(\zeta+\mu_v)}}.$$

Hence the basic reproduction number is

$$R_0 = \sqrt{\frac{\zeta\mu_h\sigma\beta_v\Gamma_v(\eta\beta_1+\beta_2(\theta+\mu_h))}{\Gamma_h\mu_v^2(\eta+\theta+\mu_h)(\sigma+\mu_h)(\gamma_h+\mu_h)(\zeta+\mu_v)}}.$$

3.4 Endemic equilibrium

The state of equilibrium in which an infection persists within a population is termed as endemic equilibrium. From the above system of equations, we get the endemic equilibrium point as follows

$$S^*_{Hh} = \frac{\eta\Gamma_h}{\beta_1\eta(\lambda_v)^* + \beta_2\theta(\lambda_v)^* + \beta_1(\lambda_h)^*\mu_h + \beta_2\lambda_h\mu_h + \beta_1\beta_2((\lambda_v)^*)^2 + \eta\mu_h + \theta\mu_h + \mu_h^2},$$

$$S^*_{Lh} = \frac{\Gamma_h\left(\beta_1(\lambda_v)^* + \mu_h + \theta\right)}{\beta_1\eta(\lambda_v)^* + \beta_2\theta(\lambda_v)^* + \beta_1(\lambda_v)^*\mu_h + \beta_2(\lambda_v)^*\mu_h + \beta_1\beta_2((\lambda_h)^*)^2 + \eta\mu_h + \theta\mu_h + \mu_h^2},$$

$$E^*_h = \frac{\Gamma_h(\lambda_v)^*\left(\beta_1\eta + \beta_2\theta + \beta_2\beta_1(\lambda_v)^* + \beta_2\mu_h\right)}{\left(\mu_h+\sigma\right)\left(\beta_1\eta(\lambda_v)^* + \beta_2\theta(\lambda_v)^* + \beta_1(\lambda_v)^*\mu_h + \beta_2(\lambda_v)^*\mu_h + \beta_1\beta_2((\lambda_v)^*)^2 + \eta\mu_h + \theta\mu_h + \mu_h^2\right)},$$

$$I^*_h = \frac{\sigma\Gamma_h(\lambda_v)^*\left(\beta_1\eta + \beta_2\theta + \beta_2\beta_1(\lambda_v)^* + \beta_2\mu_h\right)}{\left(\gamma_h+\mu_h\right)\left(\mu_h+\sigma\right)\left(\beta_1\eta(\lambda_v)^* + \beta_2\theta(\lambda_v)^* + \beta_1(\lambda_v)^*\mu_h + \beta_2(\lambda_v)^*\mu_h + \beta_1\beta_2((\lambda_v)^*)^2 + \eta\mu_h + \theta\mu_h + \mu_h^2\right)},$$

$$R^*_h = \frac{\sigma\gamma_h\Gamma_h\lambda_v\left(\beta_1\eta + \beta_2\theta + \beta_2\beta_1(\lambda_v)^* + \beta_2\mu_h\right)}{\mu_h\left(\gamma_h+\mu_h\right)\left(\mu_h+\sigma\right)\left(\beta_1\eta(\lambda_v)^* + \beta_2\theta(\lambda_v)^* + \beta_1(\lambda_v)^*\mu_h + \beta_2(\lambda_v)^*\mu_h + \beta_1\beta_2((\lambda_v)^*)^2 + \eta\mu_h + \theta\mu_h + \mu_h^2\right)},$$

$$S^*_v = \frac{\Gamma_v}{\beta_v(\lambda_h)^* + \mu_v}, E^*_v = \frac{\beta_v\Gamma_v(\lambda_h)^*}{\left(\zeta+\mu_v\right)\left(\beta_v(\lambda_h)^* + \mu_v\right)}, I^*_v = \frac{\zeta\beta_v\Gamma_v(\lambda_h)^*}{\mu_v\left(\zeta+\mu_v\right)\left(\beta_v(\lambda_h)^* + \mu_v\right)},$$

where $\lambda^*_v = \frac{I^*_v}{N^*_h}$ and $\lambda^*_h = \frac{I^*_h}{N^*_h}$.
After some algebraic manipulations with equilibrium solutions, we have

$$A(\lambda^*_v)^2 + B\lambda^*_v + C = 0 \tag{13}$$

where,

$$\begin{aligned}
A &= \beta_1\beta_2\Gamma_h\mu_v\left(\zeta+\mu_v\right)\left(\sigma\mu_h\beta_v + \mu_v\left(\gamma_h+\mu_h\right)\left(\mu_h+\sigma\right)\right)\\
B &= \beta_1\left(\Gamma_h\mu_v\left(\zeta+\mu_v\right)\left(\eta\sigma\mu_h\beta_v + \mu_v\left(\gamma_h+\mu_h\right)\left(\eta+\mu_h\right)\left(\mu_h+\sigma\right)\right) - \beta_2\zeta\sigma\mu_h^2\beta_v\Gamma_v\right)\\
&\quad + \beta_2\Gamma_h\mu_v\left(\mu_h+\theta\right)\left(\zeta+\mu_v\right)\left(\sigma\mu_h\beta_v + \mu_v\left(\gamma_h+\mu_h\right)\left(\mu_h+\sigma\right)\right)\\
C &= \left(1 - R_0^2\right)\Gamma_h\mu_h\mu_v^2\left(\gamma_h+\mu_h\right)\left(\mu_h+\sigma\right)\left(\zeta+\mu_v\right)\left(\eta+\mu_h+\theta\right)
\end{aligned}$$

Since Eq.(13) has unique positive solution λ^*_v if $R_0 > 1$ and hence the system has unique endemic equilibrium when $R_0 > 1$.

3.5 Local stability of disease free equilibrium

The Jacobian of the system (1-8) at disease-free equilibrium

$$J = \begin{pmatrix}
-\theta-\mu_h & \eta & 0 & 0 & 0 & 0 & 0 & -\frac{\eta\beta_1}{\eta+\theta+\mu_h}\\
\theta & -\eta-\mu_h & 0 & 0 & 0 & 0 & 0 & \frac{\beta_2(\theta+\mu_h)}{\eta+\theta+\mu_h}\\
0 & 0 & -\sigma-\mu_h & 0 & 0 & 0 & 0 & \frac{\eta\beta_1+\beta_2(\theta+\mu_h)}{\eta+\theta+\mu_h}\\
0 & 0 & \sigma & -\gamma_h-\mu_h & 0 & 0 & 0 & 0\\
0 & 0 & 0 & \gamma_h & -\mu_h & 0 & 0 & 0\\
0 & 0 & 0 & -\frac{\beta_v\mu_h\Gamma_v}{\Gamma_h\mu_v} & 0 & -\mu_v & 0 & 0\\
0 & 0 & 0 & \frac{\beta_v\mu_h\Gamma_v}{\mu_v\Gamma_h} & 0 & 0 & -\zeta-\mu_v & 0\\
0 & 0 & 0 & 0 & 0 & 0 & \zeta & -\mu_v
\end{pmatrix}.$$

Using the matrix J, we find the following characteristics equation

$$(\mu_h+\lambda)(\mu_h+\lambda)(\eta+\theta+\mu_h+\lambda)(\mu_v+\lambda)\left[\lambda^4 + a_1\lambda^3 + a_2\lambda^2 + a_3\lambda + a_4\right] = 0 \tag{14}$$

From the Eq.14, it is observed that four eigenvalues are $-\mu_h, -\mu_h, -\eta - \theta - \mu_h, -\mu_v$. After solving the following equation, we will get the remaining four eigen values:

$$\lambda^4 + a_1\lambda^3 + a_2\lambda^2 + a_3\lambda + a_4 = 0, \tag{15}$$

where,

$$\begin{aligned}
a_1 &= \zeta + \sigma + \gamma_h + 2\mu_h + 2\mu_v \\
a_2 &= \zeta\sigma + \zeta\gamma_h + 2\zeta\mu_h + \sigma\mu_h + \gamma_h\mu_h + \mu_h^2 + \zeta\mu_v + 2\sigma\mu_v + 2\gamma_h\mu_v + 4\mu_h\mu_v + \mu_v^2 \\
a_3 &= \sigma\mu_v(\zeta + \mu_v) + \mu_h^2(\zeta + 2\mu_v) + \mu_h(\zeta\sigma + 2(\zeta + \sigma)\mu_v + 2\mu_v^2) \\
&\quad + \gamma_h\left(\zeta\sigma + (\zeta + 2\sigma)\mu_v + \mu_v^2 + \mu_h(\zeta + 2\mu_v)\right) \\
a_4 &= \mu_v(\sigma + \mu_h)(\gamma_h + \mu_h)(\zeta + \mu_h)(1 - R_0^2).
\end{aligned}$$

Hence all a_1, a_2, a_3, a_4 are positive if $R_0 < 1$.
Also, $a_1a_2a_3 - a_3^2 - a_1^2a_4 = R_0^2\mu_v\left(\gamma_h + \mu_h\right)\left(\mu_h + \sigma\right)\left(\zeta + \mu_v\right)\left(\zeta + \gamma_h + 2\mu_h + \sigma + 2\mu_v\right)^2$
$+ \left(\zeta + 2\mu_v\right)\left(\gamma_h + 2\mu_h + \sigma\right)\left(\gamma_h + \mu_h + \mu_v\right)\left(\mu_h + \sigma + \mu_v\right)\left(\zeta + \gamma_h + \mu_h + \mu_v\right)\left(\zeta + \mu_h + \sigma + \mu_v\right) > 0$.
Thus, by Routh - Horwitz criteria, the disease-free equilibrium is locally asymptotically stable for $R_0 < 1$.

4 Results and Discussion

In this section, we analyze the trajectory of dengue disease and assess the effectiveness of various control strategies in mitigating dengue cases within Rupandehi district.

4.1 Effective reproduction number

Based on the estimated parameters, we observed the reproduction number R_0, which started at 3.6 . This initial value remained greater than unity until November 8, indicating a sustained upward trend in disease transmission. As time progressed, the epidemic is expected to shift towards a declining trend, with R_t dropping below 1. The significance of this threshold, $R_0 = 1$, lies in its ability to delineate whether an epidemic will propagate or diminish. This pivotal point is visually depicted by the inclusion of a dotted line in our analysis.

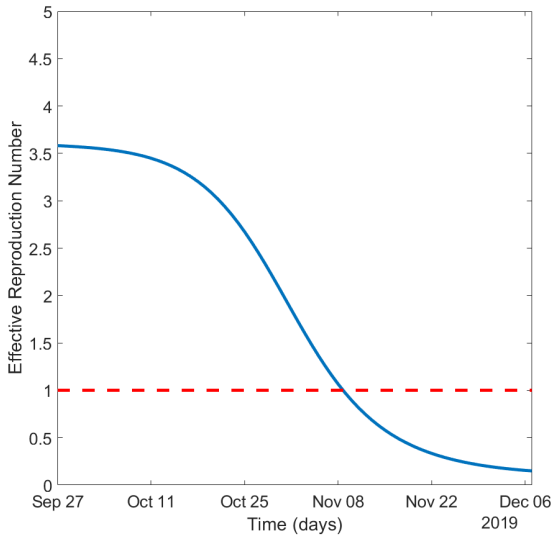

Figure 5: Trend of effective reproduction number in Rupandehi district in 2017.

4.2 Reported and non-reported cases

Figure 6 provides an overview of the reported and non-reported cases of dengue disease within Rupandehi district during the year 2017. Our analysis unveils a striking contrast between the officially documented cases and the actual occurrences. Despite the reported figures, it becomes evident that a substantial gap exists between these records and the true number of cases, indicating a significant level of underreporting. Remarkably, our estimates suggest that only 10% of the total dengue cases in Rupandehi were captured through official channels. This stark disparity underscores the magnitude of underreporting within the district, shedding light on the need for improved surveillance and reporting mechanisms to accurately assess the burden of dengue and implement timely control measures.

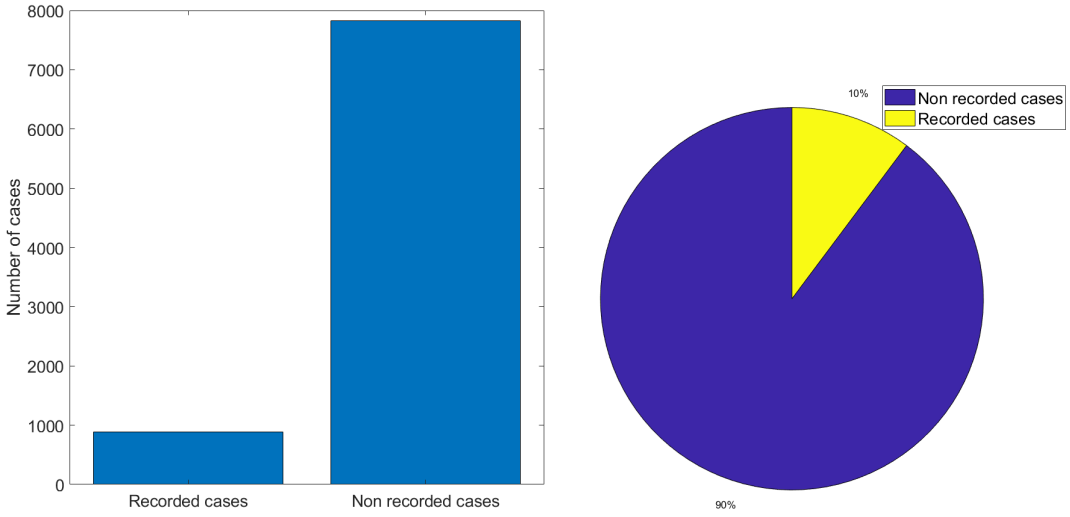

(a) (b)

Figure 6: (a) Reported and actual cases of dengue disease in Rupandehi district (b) Percentage of reported and non reported cases.

4.3 Impact of control strategies on the mitigation of dengue cases

Figures 7 and 8 depict simulations illustrating the impact of various control strategies on mitigating dengue disease. These visualizations provide insight into how adjustments in the intensity of control measures influence the trajectory of cumulative cases and daily new cases. Among the range of control strategies scrutinized, it becomes evident that the transmission rate from infectious humans to susceptible mosquitoes β_v emerges as the most influential parameter in reducing the burden of dengue cases. These simulations underscore the critical role of β_v in shaping the effectiveness of control efforts against dengue transmission.

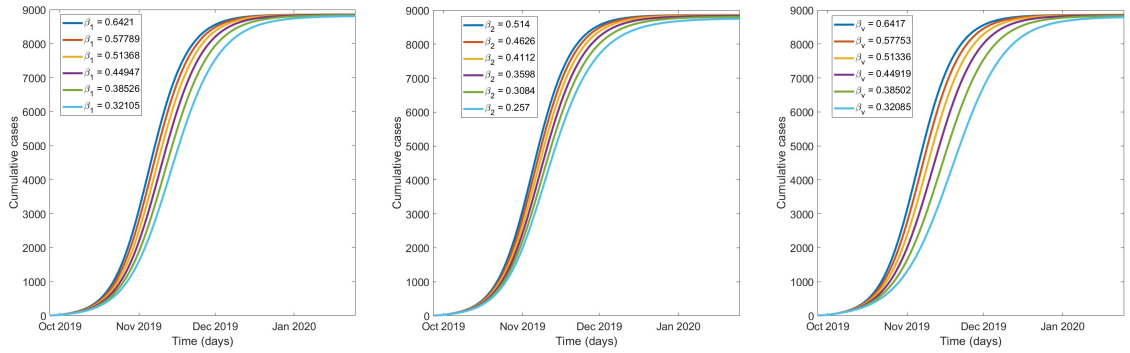

(a) (b) (c)

Figure 7: (a) Impact of transmission rate in high risk susceptible group on the reduction of size of the outbreak (b) Impact of transmission rate in low risk susceptible group on the reduction of size of the outbreak (c) Impact of transmission rate in vector on the reduction of size of the outbreak.

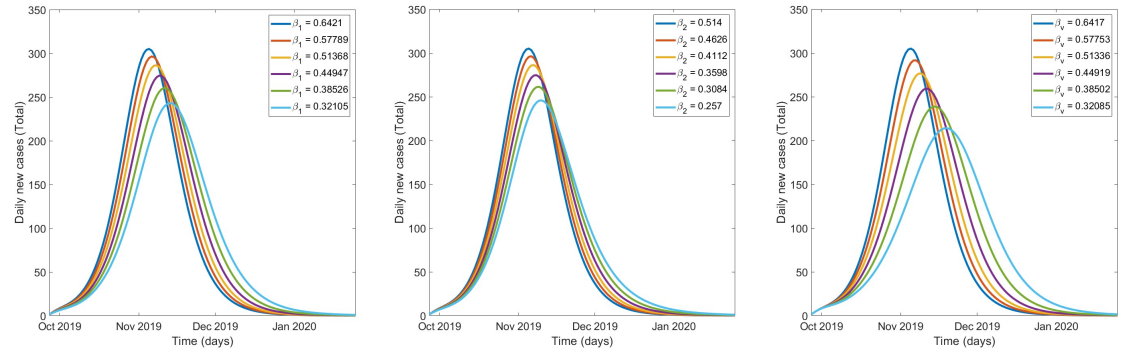

(a) (b) (c)

Figure 8: (a) Influence of transmission rate among high-risk susceptible groups on the reduction of daily outbreak cases (b) Influence of transmission rate among low-risk susceptible groups on the reduction of daily outbreak cases (c) Impact of transmission rate among vectors on the reduction of daily outbreak cases.

Figure 9 provides a visual representation of how different control strategies impact the effective reproduction number, a critical indicator of disease transmission dynamics. By examining this figure, we gain insights into how variations in control measures affect the rate at which the disease spreads within a population. Notably, β_v, the transmission rate from infectious humans to susceptible mosquitoes, emerges as particularly influential in determining the effectiveness of control efforts. This suggests that strategies targeting reduction of mosquito biting rate using Insecticide Treated Nets (ITN), have a significant impact on reducing the transmission of the disease. Understanding the sensitivity of β_v among the studied strategies underscores the importance of implementing targeted interventions aimed at reducing mosquito biting rate in dengue control programs.

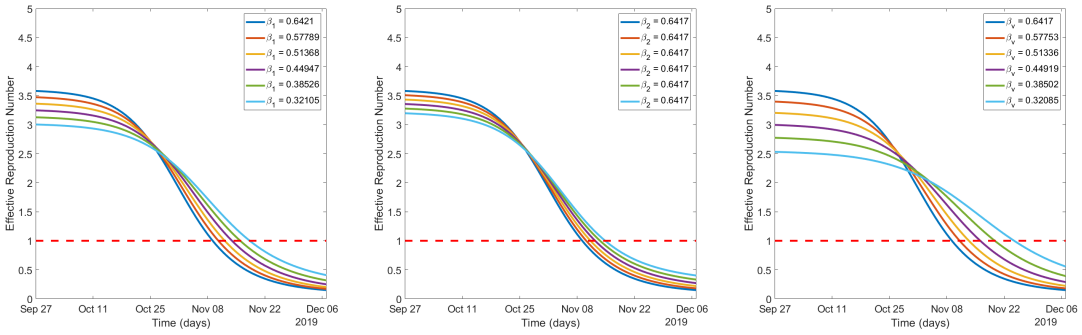

(a) (b) (c)

Figure 9: (a) Impact of transmission rate among high-risk susceptible groups on the reduction of effective reproduction number (b) Impact of transmission rate among low-risk susceptible groups on the reduction of effective reproduction number (c) Impact of transmission rate among vectors reduction of effective reproduction number.

Figure 10 explores the effects of the control approach mosquito death rate (μ_v) on the accumulation of cases, daily incidences of dengue cases, and the effective reproduction number. Based on our findings, we concluded that μ_v is the most sensitive parameter among the ones we examined. It has a greater impact compared to β_1, β_2, and β_v. Our finding highlights the vital role of μ_v in influencing the trends of dengue transmission and stresses its significance in the context of developing efficient control strategies. Increasing sensitivity of μ_v emphasizes its potential as a target for interventions targeted at reducing the transmission of dengue disease.

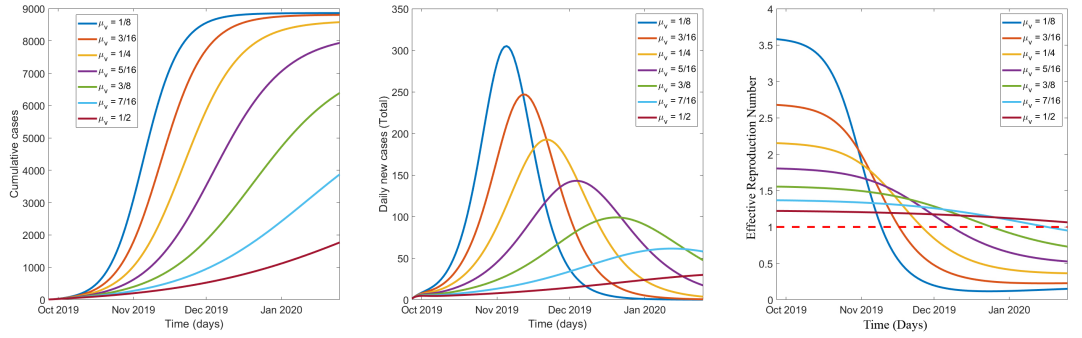

(a) (b) (c)

Figure 10: Influence of vector death rate (β_v) on the reduction of (a) Total size of the outbreak (b) Daily cases of the outbreak (c) Effective reproduction number during the outbreaks.

4.4 Local sensitivity of R_0 to the parameters

Local sensitivity method involves analyzing the impact of individual input parameters on the model output while holding all other input parameters constant. Due to its simplicity in both application and calculation, this method is commonly utilized in conventional sensitivity analyses. Sensitivity analysis plays a vital role in understanding the significance of each parameter in disease transmission. This information is essential not just for designing experiments but also for incorporating data and simplifying complex nonlinear models. It helps assess how robust model predictions are to variations in parameter values, accounting for potential errors in data collection and assumptions about parameter values. By identifying parameters

with significant impact on the basic reproduction number R_0, sensitivity analysis aids in devising targeted intervention strategies.

Sensitivity indices provide a means to quantify the relative change in a variable when a parameter varies. The normalized forward sensitivity index of a variable concerning a parameter is the ratio of the relative change in the variable to the relative change in the parameter. Alternatively, when the variable is a differentiable function of the parameter, the sensitivity index can be defined using partial derivatives.

The normalized forward sensitivity index of R_0 , which is differentiable with respect to a parameter p, is defined as [18]:

$$\Upsilon_p^{R_0} = \frac{\partial R_0}{\partial p} \times \frac{p}{R_0}$$

.

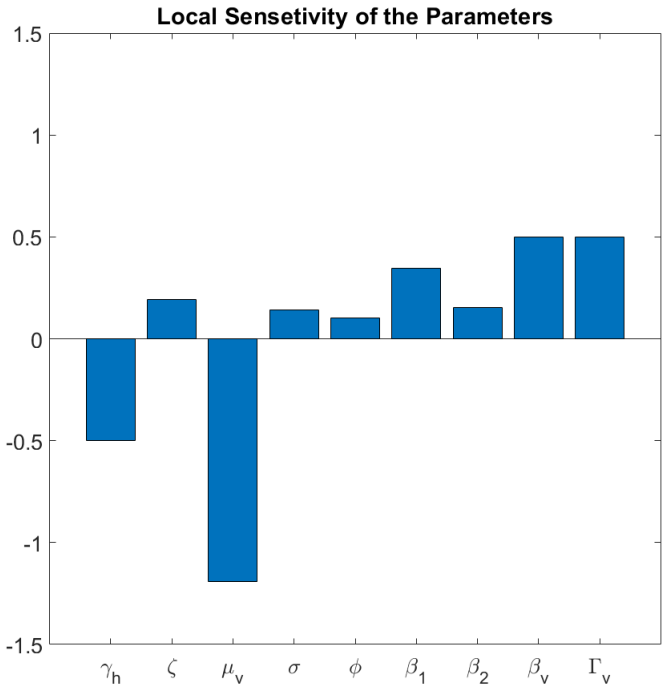

Figure 11: Local sensitivity of parameters to R_0. The sensitivity index, $\Upsilon_p^{R_0}$, showing the level of change in R_0 with respect to the parameters.

The parameters ζ, σ , ϕ, β_1 , β_2 , β_v and Γ_v exhibit positive sensitivity indices. The most positive sensitive parameters are β_v and Γ_v, while parameters γ_h and μ_v have negative sensitivity indices (Figure 11). The parameter with the most negative sensitivity index is the mosquito death rate, denoted as μ_v and its estimated value is 0.125 per day. From Figure 11, we can see that if μ_v is increased by 12.5%, then the basic reproduction number decreases by 12.5%.

5 Conclusion

In recent years, rising outbreak of dengue disease has become a significant public health challenge, particularly in poor and developing countries like Nepal. This study focusing the dengue outbreaks in Rupandehi district in Nepal. We developed a mathematical model $S_{Hh}S_{Lh}EIR - SEI$ and analysed the transmission dynamics of dengue outbreaks in Rupandehi district in 2017. We examined the basic properties of the

model to validate epidemically and biologically by proving the positivity and boundedness of solutions. The basic reproduction number is calculated to determine whether the disease dies out or persists. Moreover, we obtained the disease free equilibrium point and its stability and endemic equilibrium point. The sensitivity analysis, observed that the R_0 is highly influenced with mosquito death rate (μ_v) followed by transmission rate from infectious humans to susceptible mosquito β_v and mosquito recruitment rate Γ_v. This implies that the implementation of awareness programs about dengue disease is recommended as a preventive measure and controlling mosquito population effectively could automatically reduce dengue transmission. The study concluded that the risk of dengue disease in Rupandehi district is not worrisome, but precautions must still be taken given the absence of effective treatments for dengue. Controlling the mosquito population is also crucial, as reducing mosquito numbers can significantly lower dengue virus.

From the available data higher incidence of dengue infections among the male population compared to females. This may be attributed to the fact that males typically engage in outdoor activities during the day, as dictated by the socioeconomic structure of our society. Additionally, it was found that the active population is more susceptible to dengue infection than dependent populations, leading to adverse economic consequences for society as a whole. Moreover, we examined the impact of control strategies on the mitigation of dengue disease and found that the each and every parameter have impact on mitigation of dengue cases but μ_v has highest impact.

In summary, we developed a model of dengue transmission in the context of Rupandehi district in Nepal, and analysed impact of control strategies on the mitigation of the disease. Our analysis and the numerical simulations of the model can provide helpful information for policymakers to design programs to eradicate the disease. We acknowledge to some limitations, that the study is limited within the area of a small part of the country assuming the homogeneous population.

References

[1] Adhikari, K., Gautam, R., Pokharel, A., Uprety, K. N., and Vaidya, N. K., 2021, Transmission dynamics of COVID-19 in Nepal: Mathematical model uncovering effective controls, *Journal of Theoretical Biology*, 521, 110680. DOI: `https:doi.org/10.1016/j.jtbi.2021.110680`

[2] Adhikari, K., Gautam, R., Pokharel, A., Dhimal, M., Uprety, K., and Vaidya, N. K., 2022, Insight into delta variant dominated second wave of COVID-19 in Nepal, *Epidemics*. 41. 100642. DOI: `https:doi.org10.1016/j.epidem.2022.100642`

[3] Adhikari, K., Gautam, R., Pokharel, A., Uprety, K. N., and Vaidya, N. K., 2023, Data-driven models for the risk of infection and hospitalization during a pandemic: Case study on COVID-19 in Nepal, *Journal of Theoretical Biology*. 574. 111622. DOI: `https:doi.org10.1016/j.jtbi.2023.111622`

[4] Aguiar, M., Anam, V., Blyuss, K. B., Estadilla, C. D. S., Guerrero, B. V., Knopoff, D., Kooi, B. W., Srivastav, A. K., Steindorf, V., and Stollenwerk, N., 2022, Mathematical models for dengue fever epidemiology: A 10-year systematic review, *Physics of life reviews,* 40, 65–92. DOI: `https:doi.org/10.1016/j.plrev.2022.02.001`

[5] Chanda, N., Adhikari, K., Gautam, R., Pokharel, A., and Uprety, K., 2023, Estimating the effects of nonpharmaceutical interventions of COVID-19 in Sudurpaschim Province, Nepal, *Journal of Institute of Science and Technology*, 28. 31-43. DOI: `https:doi.org10.3126/jist.v28i1.49044`

[6] Esteva, L., and Vargas, C., 1998, Analysis of a dengue disease transmission model, *Mathematical Bio-sciences,* 150(2), 131–151. DOI: `https:doi.org/10.1016/s0025-5564(98)10003-2`

[7] Fischer, D. B., and Halstead, S. B., 1970, Observations related to pathogenesis of dengue hemorrhagic fever. V. Examination of agspecific sequential infection rates using a mathematical model, *The Yale Journal of Biology and Medicine*, 42(5), 329–349.

[8] Gautam, R., Pokharel, A., Adhikari, K., Uprety, K. N., and Vaidya, N. K., 2022, Modeling malaria transmission in Nepal: impact of imported cases through cross-border mobility, *Journal of Biological Dynamics*, 16(1), 528–564. DOI: https:doi.org/10.1080/17513758.2022.2096935

[9] Gubler D. J., 1998, Dengue and dengue hemorrhagic fever, *Clinical Microbiology Reviews*, 11(3), 480–496. DOI: https:doi.org/10.1128/CMR.11.3.480

[10] Jose, S., Raja, R., Omede, B., Agarwal, R. Alzabut, J., Cao, J., and Balas, V., 2022, Mathematical modeling on co-infection: transmission dynamics of Zika virus and Dengue fever, *Nonlinear Dynamics,* 10.1007/s11071-022-08063-5

[11] Joseph D, Ramachandran R, Alzabut, J., Jose, S,.and Khan, H., 2023, A fractional-order density-dependent mathematical model to find the better strain of Wolbachia, *Symmetry*, 15(4):845. DOI: https:doi.org/10.3390/sym15040845

[12] Kafle, J., Bayalkoti, P., and Phaijoo, G. R., 2023, Mathematical study of effect of temperature on transmission dynamics of dengue disease, *Journal of Nepal Mathematical Society,* 6(1), 34–47. DOI: https://doi.org/10.3126/jnms.v6i1.57476

[13] Kermack, W. O., and McKendrick, A. G., 1927, A contribution to the mathematical theory of epidemics, *Proceedings of the Royal Society of London*, Series A, Containing papers of a mathematical and physical character, 115(772), 700-721.

[14] Phaijoo, G. R., and Gurung, D. B., 2017, Mathematical model of dengue disease transmission dynamics with control measures, *Journal of Advances in Mathematics and Computer Science*, 23(3), 1-12.

[15] Pokharel, A., Adhikari, K., Gautam, R., Uprety, K., and Vaidya, N. K., 2024, Modeling measles transmission in adults and children: Implications to vaccination for eradication, *Infectious Disease Modelling.* DOI: https:doi.org10.1016/j.idm.2024.04.012

[16] Pokharel, P., Khanal, S., Ghimire, S., Pokhrel, K. M., and Shrestha A. B., 2023, Frequent outbreaks of dengue in Nepal – causes and solutions: a narrative review *International Journal of Surgery Global Health*, Vol. 6. No. 5.

[17] Rahman, M., Bekele-Maxwell, K., Cates, L. L., Banks, H. T., and Vaidya, N. K., 2019, Modeling Zika virus transmission dynamics: parameter estimates, disease characteristics, and prevention. *Scientific Reports*, 9(1), 10575.

[18] Rodrigues, S. H. Monteiro, M. T. T, and Delfim F. M., 2013, Sensitivity analysis in a dengue epidemiological model, *Conference Papers in Mathematics*. 2013. https:doi.org 10.1155/2013/721406

[19] Rodrigues, H. S., Monteiro, M. T. T., Torres, D. F. M., and Zinober, A., 2012, Dengue disease, basic reproduction number and control, *International Journal of Computer Mathematics,* 89(3), 334–346. DOI: https:doi.org/10.1080/00207160.2011.554540

[20] Vaidya, N. K., and Wang, F. B., 2021, Persistence of mosquito vector and dengue: Impact of seasonal and diurnal temperature variations, *Discrete and Continuous Dynamical Systems* - Series B. 27. DOI: https:doi.org10.3934/dcdsb.2021048

[21] District Public Health Office (DPHO) of Rupandehi, Nepal, 2070, *Annual Report.*

[22] Central Bureau of Statistics, Nepal, 2011, *Census of Nepal 2011*,Volume 06, NPHC2011.

[23] Epidemiology and Disease Control Division, Government of Nepal, 2022, *Situation Updates of Dengue.* Available at: https:edcd.ekbana.info/news/download/situation-updates-of-dengue-asof-15-oct-2022 (Accessed Oct 16, 2022).

[24] Health Management Information System Database,Nepal, 2017/18 , *Annual Report*, dohs.gov.np. http:dohs.gov.np/wp-content/uploads/2019/07/DoHS-Annual-Report-FY-2074-75-date-22-Ashad-2076-for-web-1.pdf

[25] National Guidelines on Prevention, Management and Control of Dengue in Nepal, 2019, *Department of Health Services Epidemiology and Disease Control Division*

[26] National Planning Commission, Government of Nepal, 2014, *Nepal Human Development Report*, Singha Durbar, Kathmandu, Nepal.

[27] World Health Organization, 2022, Dengue and severe dengue,https:www.who.int/newsroom/fact-sheets/detail/dengue-and-severe-dengue#:~:text=The%20global%20incidence%20of%20dengue,on%20effective%20vector%20control%20measures